

# Compact Low-cost Scanner for 3D-Reconstruction of Body Parts with Structured Light Illumination

Andreas Tortschanoff, Andreas Fritz and Raimund Leitner

Carinthian Tech Research AG, Europastrasse 4/1, 9524 Villach, Austria  
[andreas.tortschanoff@ctr.at](mailto:andreas.tortschanoff@ctr.at)

## Abstract

*This paper describes a low-cost miniaturized 3D reconstruction approach using structured light. By projecting known patterns onto a surface, shape and structure of the surface can be measured and characteristic parameters of deformation can be determined. Existing approaches use large geometries and complex optical components. Here we present our system with the size of a cigarette pack and a working distance of only 6 cm. The theoretical depth resolution of the system is determined by the resolution of the camera and the projector as well as the system geometry and was found to be about 100  $\mu\text{m}$ .*

**Keywords:** 3D reconstruction, structured light, miniaturized, low-cost, Gray code

## 1. Introduction

Besides traditional applications like face- and body 3D-measurement e.g. for person recognition or esthetic surgery, there is an increasing demand for high resolution 3D-reconstruction of body parts. Applications in this context [i] include the investigation of skin roughness [ii] and wrinkles [iii], scar- and wound measurements[iv,v], as well as the characterization of acne, cellulite, or psoriasis[vi]. In such cases 3D-data can provide additional quantitative information in order to characterize the situation and potential changes in an objective way, independent of texture or the subjective visual assessment of an investigator.

Different approaches exist for this kind of measurements, split up mainly into passive methods like stereo reconstruction and active methods like laser range finders[vii]. Laser range finders tend to be expensive and, as a consequence, very often the technology of passive stereo reconstruction with two cameras is used for low-cost solutions. A drawback of this method is the difficulty of finding the point correspondences. Even for sophisticated image processing algorithms it is hard to overcome certain problems like unstructured surfaces where points of interest are very difficult to identify. To solve these issues an active stereo reconstruction approach can be used based on structured light illumination. In this approach one camera is replaced by a projector projecting known patterns onto a scene. These patterns can be used to find the point correspondences without any further time consuming and complex image processing steps. There also exist different patterns which can be used for the structured light approach. The optimal pattern depends on the intended use of the system. (E.g. using a coloured pattern requires the surface under inspection not to corrupt the colour which would lead to a false detection.) Inspection time is another point which has to be taken into account. Using a series of patterns where any of them is a refinement of the previous one may take longer than a single projected pattern, but the latter has the drawback of complex image processing needs.

In this work an active stereo vision system based on structured light will be presented. Existing approaches [viii,ix] often are rather bulky in order to achieve the required optical specifications and in general they tend to be rather expensive.

The goal of this work was to develop a low-cost hand held device using structured light for the 3D reconstruction which could be used for limb, wound or scar measurements. Because measurement time is not the primary criterion for the prototype Gray coded patterns are used, meaning a series of images where each image is a refinement of its predecessor one.

In the following we describe in much detail our implementation and show first results.

## **2. Set-up**

### **2.1. Hardware**

For a structured-light stereo system an active projector and a camera have to be combined. In this project the DLP Pico Projector Development Kit of Texas Instruments was used, which has a dimension of 45mm x 47mm x 14mm. For the communication a HDMI and an I2C port are available. For this project the HDMI port is used and the projector was set as a second monitor. An important point is to project the image in full screen which is recommended for the structured light approach because otherwise there will be a loss in resolution. This cannot be done directly in MatLab but there exist scripts and toolboxes to overcome this problem using different libraries. In this project a library from the Matlab file exchange [x] based on JAVA is used.

The projector has a resolution of 480 x 320 pixels and includes red, green and blue light emitting diodes (LED) for visible light. The projector has to be set as a second monitor with a resolution of 640 x 480 pixels but internally the resolution is decreased to the maximum projector resolution. For the finest pattern the scaling factor has to be considered because this leads to a wrong representation of patterns caused by an uneven stripe width. As a workaround the pattern has been generated for a resolution of 480 x 320 pixels and afterwards can be resized to 640 x 480 pixels and sent to the projector.

For the camera module a Huentek HUAF301A is used. This miniaturized camera module is commonly used for handy or laptop cameras. The array size of the camera chip is 2048 x 1536 pixels resulting in a 3.2 Mega pixel camera. The pixel size is 1.75  $\mu\text{m}$  and the focal length is 3.42 mm. The voltage supply as well as the data transfer is performed over USB.

This camera has no auto focus which is a required specification for the reconstruction. An auto focus changes the focal length over the acquisition, so the system has to be calibrated for each acquisition which is impracticable. Also the back light compensation, the exposure mode and white balancing has to be set manually for the correct extraction of Gray patterns.

### **2.2. Implementation**

The aim was to realise a low-cost hand held device. To receive a small model with the appropriate angle and baseline the camera is rotated 90 degrees with respect to the projector. Also the projector is displaced behind the camera because of the minimal working distance of the projector. Both, the camera and the projector are fixed on a single rack in order to obtain a rigid and robust setup which is required for the reconstruction.

Figure 1 shows the prototype mounted on a holding with a specific working distance to the object under inspection together with a reference target in front of it. Figure 1a shows the open prototype with the camera module (1) and the projector (2). The camera is normal to the object under inspection while the projector has an angle of 25 degrees. Polarisation filters are mounted in front of the camera and the projector. These filters are used to reduce total

reflection in the images. Figure 1b shows the prototype in its housing (with the cover removed).

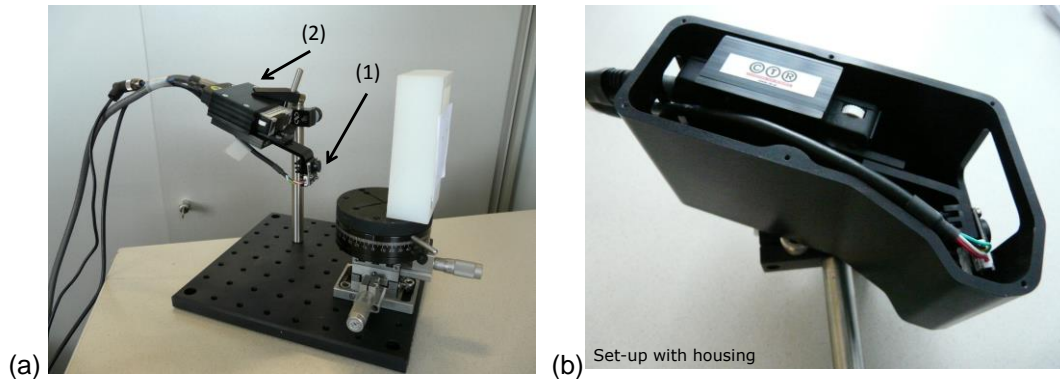


**Figure 1. The Prototype Set-up (a) Bare Set-up Including Camera, Projector and Target (b) Set-up in its Housing**

### 3. Calibration of the System

Calibration is an important part in 3D reconstruction because with an uncalibrated system no quantitative information about the actual depth or height can be obtained. The calibration of a camera system is a well-known process and there also exists a Matlab toolbox [xi] making the task of calibration easier. In this toolbox a pinhole camera model is assumed.

#### 3.1. Calibrating the Camera

In this step a set of 10 to 20 images of a checker board pattern with a well-defined size of each square has to be captured. An arbitrary rotation and translation (different to the previous ones) should be guaranteed for each captured image in order to obtain an adequate calibration result. Fundamentally there have to be at least six point correspondences to solve the equation system.

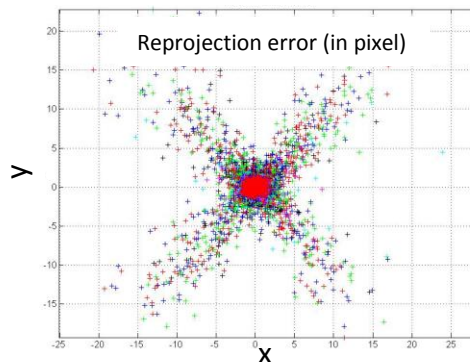


**Figure 2. The re-Projecting Error Graph for the Camera Given by the Camera Calibration Toolbox**

After the acquisition of all images the four outermost corners have to be selected and in the first image the side length of the squares has to be set. With these selected point-

correspondences the calibration can be performed and we obtain the intrinsic and extrinsic parameters of the camera.

After calibrating the camera the skew factor is zero while a re-projecting error of 1.88 px in x-direction and 1.99 px in y-direction occurs. The focal length and the principal point are listed in Table 1. The uncertainties are three times the standard deviation of the errors of estimation.

**Table 1. The Camera Calibration Parameters Given in Pixels**

	X-direction	Y-direction
Focal length	2404±15	2396±14
Principal point	821±5	1073±8

### 3.2. Calibration of the Projector

For the projector calibration a set of 10 to 20 images with arbitrary rotation and translation is captured. The main distinction between the images of camera calibration and projector calibration is that in the projector calibration the checker board pattern is projected by the projector onto a flat surface and four markers (fiducials) attached to the surface are used to define the position of the surface. Thus it is possible to obtain a relation between the projector coordinate system and the camera coordinate system.

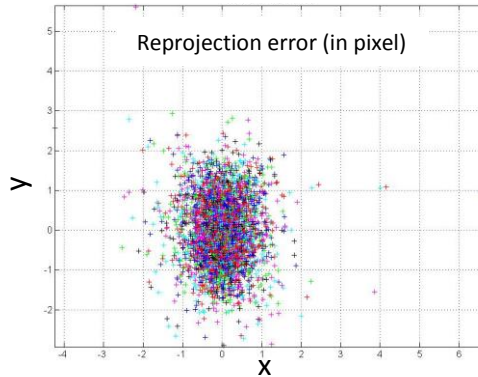


**Figure 3. The Re-projecting Error Graph for the Projector given by the Camera Calibration Toolbox**

After calibrating the projector a re-projecting error of 0.58 px in x-direction and 0.86 px in y-direction was observed in our system. The focal length and the principal point offset are listed in Table 2. The re-projecting error graph of the Camera Calibration Toolbox is shown in Figure 3.

**Table 2. The Camera Calibration Parameters Given in Pixels.**

	X-direction	Y-direction
<b>Focal length</b>	3610±96	3819±97
<b>Principal point</b>	821±5	1073±8

### 3.3. Calibration of the Stereo System

After the calibration of both, the camera and the projector, the camera coordinate system refers to the world coordinate system and the projector coordinate system as well as the object coordinate system is related to the camera coordinate system. Figure 4 shows the final calibrated system. The world coordinate system is set to the camera coordinate system meaning that the camera (red) is in the origin of the world coordinate system. The projector (green) is located behind the camera. Also the calibration targets (red for the camera and green for the projector) are shown in the figure. In this setup the system is calibrated for a working distance of 63mm.

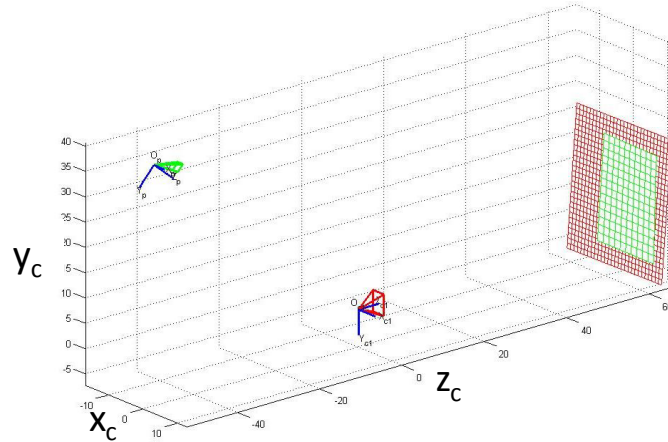


**Figure 4. The Configuration of the Calibrated Stereo Vision System. The Camera (red) is Placed at the Origin. Relating to this the Origin of the Projector is Placed behind the Camera (green). The Object is Placed in a Distance of 63mm Away from the Origin. The Checker Boards for Calibration are shown in Red for the Camera and in Green for the Projector**

To increase the speed of reconstruction the planes for each projector column and row and also the corresponding rays for each pixel are pre-calculated. This is possible as long as there is no change in the setup.

## 4. 3D-Reconstruction

### 4.1. Reconstruction of a 3D Surface

The reconstruction is split into two main parts. First, the acquisition and second the reconstruction. In the acquisition the Gray coded patterns are generated and projected onto the scene. For each projected pattern a corresponding image is acquired.

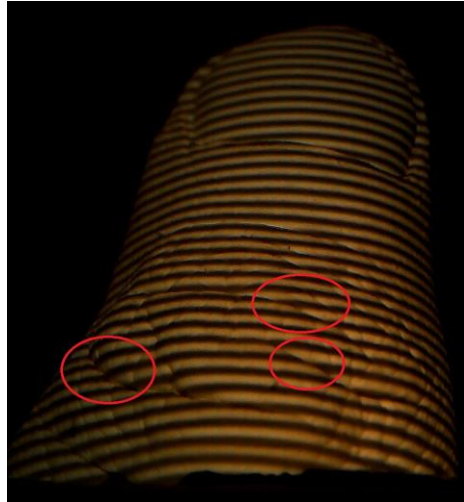


**Figure 5. One Image in the Acquisition Sequence with a Horizontally Projected Gray Pattern on a Thumb Model. In the Circled Areas the Deformation of the Projected Lines can be Seen**

For shadow correction also a fully illuminated and a background image without illumination are acquired. Hence, a total number of

$$o_{total} = 2(\log(o_{row}) + \log(o_{column})) + 2$$

pictures have to be acquired, where  $o_{row}$  and  $o_{column}$  denote the number of rows and columns of the projector respectively. Each image contains a refinement of the previous one using the Gray code. The factor of two results from inverting each Gray code pattern to overcome problems, which are caused by shadowed areas. [xii]

Figure 5 shows one image of the series for the reconstruction with a horizontal Gray pattern. At the red circled areas the deformation of a straight line that is caused by the surface of the object under inspection, can be seen.

After image acquisition the object reconstruction is performed. The reconstruction is split up into three main parts: (i) Load captured images, (ii) Extract the bit sequence from the images, and (iii) Intersect the rays from the camera pixels with the projector planes

In the extraction step each image is converted to a binary image and afterwards an XOR operation is performed on each pixel. With the resulting matrix the bit sequence can be converted into decimal values which will be used for the selection of the appropriate projector plane.

In the intersection step the intersection between the corresponding ray and projector plane is calculated for each well-defined pixel, delivering the 3D coordinate of this point.

Intersecting all pixels results in a 3D point cloud. With the 3D point cloud a triangulation on the points can be performed to fill holes and to obtain a complete surface. Finally the texture of the original image is overlaid.

In order to verify the quality of 3D reconstruction, a calibration target was fabricated, which consist of a planar surface with grooves of different depths. As can be seen in Figure 6 grooves down to a size of 100  $\mu\text{m}$  can be measured reliably on the calibration target.

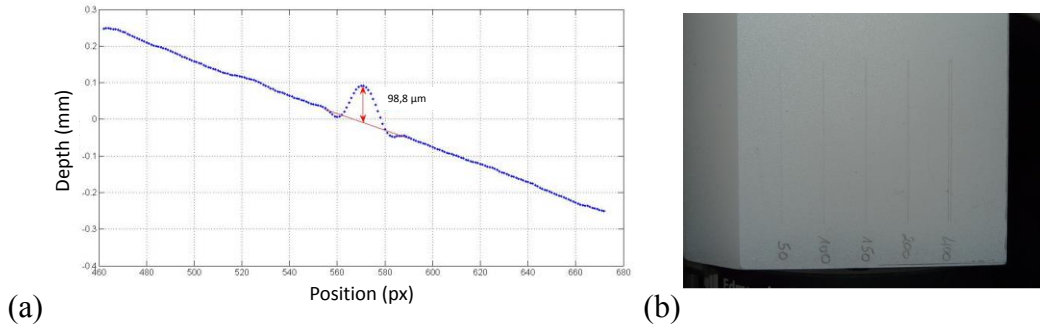


**Figure 6. (a) Cross Section of the 3D reconstruction of the Calibration Target. The Groove with a Height of 100  $\mu\text{m}$  can Clearly be Measured. (b) Photo of the Calibration Target**

## 4.2. Reconstruction of Body Parts

In this section some first reconstruction results are presented. In the first tests we used clay models, because the main issue was the demonstration of the principle and a characterization of the 3D-reconstruction performance of our set-up. In addition we show reconstruction results from a real human palm, which demonstrate the feasibility of real world measurements.

The use of models facilitates the measurement. First of all they do not move. In our initial prototype acquisition times were on the order of tens of seconds, mainly because projection and image acquisition by the camera were not specifically synchronized. Thus, at the current stage, we use a sequential data acquisition, where we allocate generous time delays (on the order of 100 ms) between the projection of a new pattern and the subsequent image acquisition. Furthermore all routines are coded in Matlab. This can be optimized and we expect that under favorable conditions acquisitions times of less than a second should be feasible using the same hardware in combination with an optimized software.

In addition, skin typically is partially transmissive for light, in particular on the red edge of the spectrum, so sharp edges become blurred during the acquisition, which can be a major obstacle in obtaining accurate Gray code images. These problems depend on the surface properties and are absent for measurements using a clay model, which has less or at least well defined and more homogeneous surface texture.

Reducing the ambient light and adapting the camera parameters it is possible to acquire human body parts, which is demonstrated with the last data set below.

**4.2.1. Thumb model:** Figure 7 shows the 3D reconstructed point cloud and the depth profile from a measurement performed with a clay model, which was generated as an exact copy of the thumb of one of the authors.

Figure 7(b) shows the cut through the above image. In this picture the fingernail region extends approximately from pixel 830 to pixel 1100. The step between the fingernail and the skin is 850  $\mu\text{m}$  which can easily be resolved.

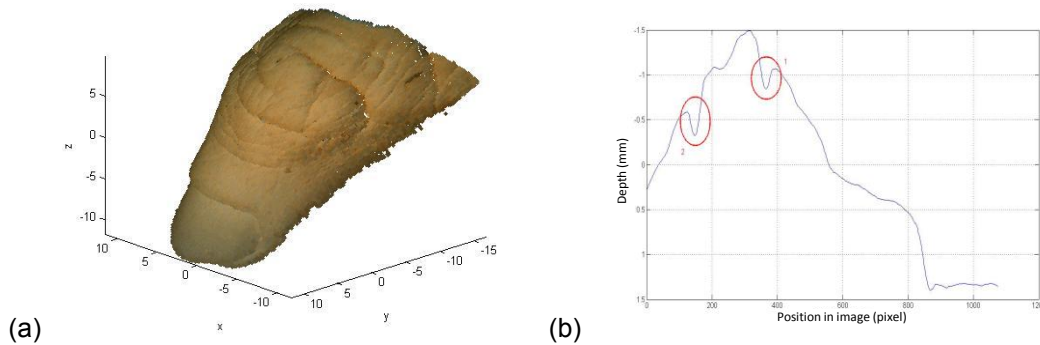


**Figure 7. (a) The 3D Point Cloud and (b) the Depth Profile of the Thumb Model. The Two Wrinkles have a Depth of 221  $\mu\text{m}$  and 261  $\mu\text{m}$ , Respectively. The Height between the Fingernail and the Skin is 850  $\mu\text{m}$**

In addition the position of two wrinkles with depths of 221  $\mu\text{m}$  and 261  $\mu\text{m}$ , respectively, is highlighted. Our miniaturized set-up can clearly resolve these features and, in combination with intelligent 3D-image processing, should be able to automatically classify and characterize similar features (wrinkles, scars, wounds,...) with high accuracy.

**4.2.2. Palm Model:** Figure 8 was taken from the model of a human hand where a small part of the palm is zoomed out. At this location one big wrinkle is present, which can clearly be quantified in the 3D-measurement. The model was taken from a widely opened hand which flattens out the wrinkles, but still this major wrinkle is visible with a depth of 818  $\mu\text{m}$ .

This dataset highlights the capabilities and possible synergies of the 2D-color image and the 3D-data. The features from wrinkles and pores and generally speaking the skin texture is clearly visible in the color image (which is overlaid on the 3D-model). On the other hand, the depth of the structures (meaning quantitative 3D information) can be unambiguously determined from the 3D-data, obtained by structured light illumination.

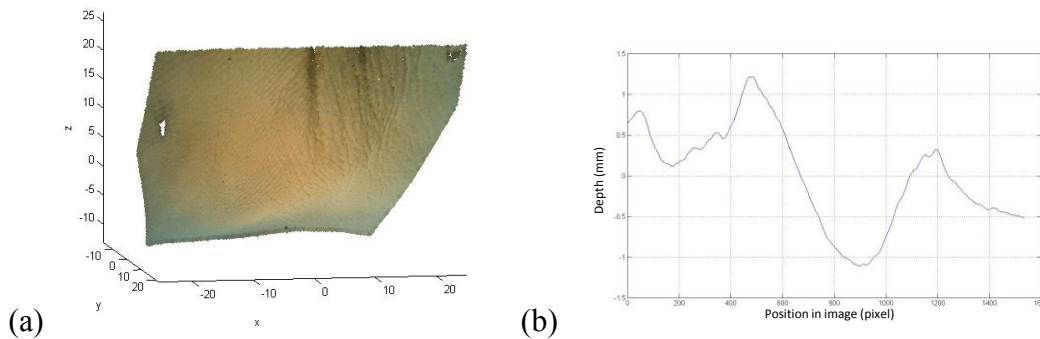


**Figure 8. (a) The 3D Point Cloud and (b) the Depth Profile of the Palm model. The Depth of the Wrinkle is 818  $\mu\text{m}$**

Again, we can stress, that we obtain a resolution in the sub-mm regime, which was the initial requirement for our set-up.

**4.2.3. Human Palm:** Finally we tested data acquisition on a real human palm. To acquire a well illuminated image of a human palm, the ambient light is eliminated. After reconstruction

two dominant wrinkles can be identified. The depth of the first wrinkle is 1.2 mm and of the second 1.3 mm. The 3D point cloud and the depth profile can be seen in Figure 9.

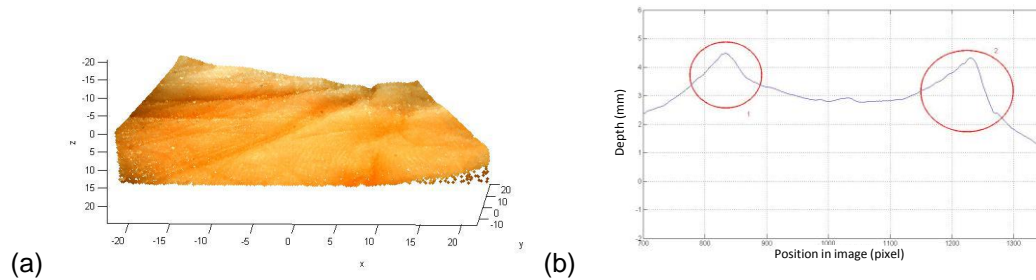


**Figure 9. (a) The 3D point Cloud and (b) the Human Palm. The Depth of the Wrinkles are 1.21 mm and 1.3 mm, Respectively**

## 5. Conclusions

In this article we presented our prototype for 3D-imaging of body parts based on the method of structured light illumination. The final prototype has a working distance of 6 cm and with its geometry it can be used as a hand held device. We successfully deployed such a prototype and developed the algorithm for reconstructing a 3D surface. We performed the calibration and the reconstruction on reference targets to evaluate the prototype and, as a first test, we reconstructed a thumb and a palm model as well as a human palm.

Because of the limited light intensity and the light absorption property of the human skin the reconstruction of human body parts needs further improvements on the prototype to deal with non-stationary surfaces and the specific scattering properties of human skin. Nevertheless, by reducing the ambient light the palm of a human hand was measured with excellent data quality. Further tests will be performed in the near future in order to evaluate the performance of our system and to confirm the first results.

## Acknowledgements

This work was funded by the Austrian COMET - Competence Centres for Excellent Technologies Programme.

## References

- [i] R.V. dos Santos, A. Mlynek, H.C. Lima, P. Martus and M. Maurer, *Clinical and Experimental Dermatology*, (2008), vol. 33, pp. 772-775.
- [ii] P. M. Friedman, G. R. Skover, G. Payonk, A. N. B. Kauvar and R. G. Geronemus, *Dermatologic Surgery*, vol. 28, no. 3, (2002), pp. 199-204.
- [iii] B. Kardorff, M. Menzinger, P. Dorittke and K. Medizin, vol. 3, no. 10, (2010).
- [iv] T. Fujimura, K. Haketa, M. Hotta and T. Kitahara, *International Journal of Cosmetic Science*, vol. 29, (2007), pp. 423-436.
- [v] F. Bernardini and H. E. Rushmeier, *Computer Graphics Forum*, vol. 21, no. 2, (2002), pp. 149-172.
- [vi] M.H. Ahmad Fadzil, E. Prakasa, H. Fitriyah, H. Nugroho, A. M. Affandi and S.H. Hussein, *World Academy of Science, Engineering and Technology*, vol. 63, (2010).
- [vii] R. Chen, G. M. Brown, M. Song, *Opt. Eng.*, vol. 39, no. 1, (2000), pp. 10-22.
- [viii] <http://www.breuckmann.com/bodymetrie-life-science>, (2012).
- [ix] <http://www.gfm3d.com>, (2012).
- [x] <http://www.mathworks.com/matlabcentral/fileexchange/11112-fullscreen>, (2012).
- [xi] [http://www.vision.caltech.edu/bouguetj/calib\\_doc/](http://www.vision.caltech.edu/bouguetj/calib_doc/), (2012).
- [xii] G. Taubin and D. Lanman. "Build your own 3d scanner: 3d photography for beginners", (2009).

